Revista de Informática Teórica e Aplicada - RITA - ISSN 2175-2745
Vol. 33, Num. 3 (2026) 109-122

RESEARCH ARTICLE

Attribute-Based Recurrent Neighbors for Dynamic Network Visualization

Vizinhos Recorrentes Baseados em Atributos para Visualização de Redes Dinâmicas

Lorena Ferreira Marani[1], Bruno Augusto Nassif Travençolo[1], José Gustavo S. Paiva[1]*

Abstract: Dynamic networks describe interactions between entities under study within a specific context over a period of time. These networks consist of nodes, which represent individual elements, and edges, which indicate interactions between those elements at each temporal instant. Within the network structure, various properties can be assigned to nodes (such as degree and centrality) and to edges (such as link strength and direction). To support the analysis of the phenomena embedded in these networks, the field of Data Visualization offers techniques that create visual representations aimed at highlighting connection patterns and assisting users in exploring these phenomena. Although widely used, such techniques often disregard node attributes, focusing solely on existing connections. However, these attributes may carry valuable information that can help in understanding interactions and even contribute to predicting future connections. To address this gap, this work extends the Recurrent Neighbors technique by incorporating node attributes into the node ordering process. The proposed approach provides a visualization strategy focused on identifying relationships between attributes and connections, aiming to enhance the understanding of factors that influence the evolution of interactions over time. The method was applied to two datasets that recorded social interactions among baboons, and our results demonstrate that ordering nodes based on their attributes improves the interpretability of dynamic networks, revealing social organization patterns that would likely go unnoticed in conventional visual representations.
Keywords: temporal networks — visualization — dynamic networks — multivariate networks

Resumo: Redes dinâmicas descrevem interações entre objetos de estudo, em determinado contexto, ao longo de um período de tempo. Essas redes são compostas por nós, que representam elementos individuais, e arestas, que indicam interações entre esses elementos em cada instante temporal. No âmbito da rede, diferentes propriedades estruturais podem ser atribuídas aos nós (como grau e centralidade) e às arestas (como força da ligação e direção). Para facilitar a análise dos fenômenos envolvidos nessas redes, a área de Visualização de Dados propõe técnicas que criam representações visuais capazes de destacar padrões de conexão e auxiliar os usuários na exploração desses fenômenos. Embora amplamente aplicadas, essas técnicas geralmente desconsideram os atributos dos nós, focando apenas nas conexões existentes. No entanto, tais atributos podem carregar informações valiosas que podem auxiliar a compreender as interações e até auxiliar na previsão de novas conexões. Para preencher essa lacuna, este trabalho estende a técnica *Recurrent Neighbors*, incorporando atributos dos nós no processo de ordenação. A proposta representa uma estratégia de visualização voltada à identificação de relações entre atributos e conexões, com foco na compreensão dos fatores que influenciam a evolução das interações ao longo do tempo. O método foi aplicado a duas bases de dados que registram interações sociais entre babuínos, e os resultados mostram que ordenar os nós com base em atributos melhora a interpretação das redes dinâmicas, revelando padrões de organização social que passariam despercebidos em representações convencionais.
Palavras-Chave: redes temporais — visualização — redes dinâmicas — redes multivariadas

[1] *Faculdade de Computação, Universidade Federal de Uberlândia (UFU), Brazil*
***Corresponding author**: Bruno Travençolo - travencolo@gmail.com
DOI: http://dx.doi.org/10.22456/2175-2745.148445 • **Received:** 27/06/2025 • **Accepted:** 18/05/2026
CC BY-NC-ND 4.0 - This work is licensed under a Creative Commons Attribution-NonCommercial-NoDerivatives 4.0 International License.

1. Introduction

Complex systems can be modeled as networks in which elements are represented by nodes and their interactions by edges. Such complex networks exhibit emergent properties that cannot be understood solely by analyzing individual components, requiring investigation of the global topology [1]. This modeling approach has been widely applied across diverse fields, including healthcare [2] and economics [3]. Network structures often evolve over time, characterizing them as Dynamic Networks (DNs) [4, 5]. Observing the temporal aspects of Dynamic Networks enables the identification of patterns, transitions, and anomalous behaviors that would remain imperceptible in static representations. The nodes in these networks may carry attributes that describe intrinsic characteristics of the represented entities in addition to topological properties such as degree and centrality. Edges, in turn, may include weights that quantify the intensity or relevance of interactions. The presence of attributes associated with both nodes and edges classifies these structures as Dynamic Multivariate Networks (DMNs) [6]. Beyond topological properties, the intrinsic attributes of nodes can significantly influence the formation and evolution of connections, demanding analytical methods that integrate both network structure and associated information. Interpreting network phenomena through purely descriptive data, however, remains a challenging task. In this context, Data Visualization techniques are essential, making such information more accessible and facilitating the identification of patterns and the understanding of underlying dynamics through visual representations [7]. Current approaches, such as DyNetVis [8, 9, 10], have yet to adequately incorporate node attributes into *layout* construction, thereby limiting visual analysis. Although some initial efforts toward DMN visualization exist [6], these solutions remain incipient, underscoring the need for advances in the integration of topology, attributes, and temporal dynamics.

In light of these limitations and the demand for more comprehensive approaches, this work proposes the development of a visualization strategy for dynamic multivariate networks that incorporates node attributes into the visual ordering process, with the aim of improving DMN interpretability and reducing the visual complexity of the *layout*. Beyond visual ordering, node coloring is employed as a complementary technique to represent variations in selected attributes, enhancing the perception of patterns and differences. For numerical attributes, a continuous gradient is applied; for categorical attributes, distinct and contrasting colors are used.

Two datasets of *Papio papio* interactions collected at the CNRS Primatology Centre in *Rousset-sur-Arc*, France [11, 12] were analyzed. Attribute-based orderings revealed social patterns — such as the centrality of older individuals and affinity-based groupings — and in some cases also reduced visual overlaps.

2. Fundamental Concepts

Complex Networks are schematic representations of complex systems grounded in Graph Theory. Unlike traditional graphs, however, these networks exhibit non-uniform characteristics such as node clustering and variations in degree distribution. A node represents an individual entity, while an edge denotes a connection or link between two nodes, which may be directed or undirected. Furthermore, both nodes and edges may carry associated properties, such as weight (relationship intensity), degree (number of connections), clustering coefficient (connections among neighbors), diameter (maximum distance between nodes), and k-core number (participation in densely connected regions), along with metrics such as eigenvector centrality, which assess the importance and influence of nodes within the network [1].

Within the scope of Complex Networks, Dynamic Networks describe the temporal evolution of nodes and their connections, exhibiting structural or contextual changes over time, such as variations in connections or community formation. Representing a system as a dynamic network enables the analysis of its behavior and the identification of interdependencies among its components. Converting this representation into a static structure, however, results in the loss of essential information regarding the order and simultaneity of events, compromising representational fidelity and potentially leading to misinterpretations [4, 5].

At a broader level, a Dynamic Multivariate Network is defined as a structure that, in addition to the temporal aspects of a Dynamic Network, also incorporates the characteristics of a Multivariate Network (i.e., additional information associated with nodes and edges). Exploring this type of network enables a deeper understanding of the data, as attributes constitute a valuable source of information capable of explaining relationships among elements and revealing intrinsic network patterns.

3. Network Visualization

Network visualization is a fundamental approach for exploring and interpreting complex and multivariate data [7]. This section presents the main *layout* techniques for dynamic and multivariate networks, emphasizing the importance of incorporating node attributes into the visualization process.

3.1 Traditional Network Layouts

A range of visualization layouts have been proposed to address different analytical needs in dynamic and multivariate networks:

1. **Node-Edge Diagrams:** represent nodes as points and edges as lines [13]. Although intuitive, they tend to become visually cluttered in dense networks.
2. **Adjacency Matrices:** arrange nodes in rows and columns, with cells indicating connections [14]. Effective for large networks and for the identification of clusters.

3. **Temporal Activity Maps (TAM):** visualize node activity over time through color-coded intensities [15].
4. **Sequence View (SV):** arranges nodes in horizontal lines and represents connections as vertical lines across time intervals [16], enabling the detection of dynamic patterns and periodicity.
5. **Overview + Detail Techniques (minimaps):** provide compact versions of the main layouts to supply context and support user navigation [17].
6. **Attribute-guided layouts:** position nodes based on shared characteristics (e.g., language or centrality), revealing clustering patterns beyond network topology [18].

Despite significant advances, only a few approaches explicitly incorporate node attributes into layout generation. This limitation reduces the interpretive power of visualizations, particularly in DMNs, where attribute information is central to the observed dynamics. Most existing studies focus on either temporal aspects or node attributes, frequently neglecting a comprehensive integration of both. More effective and intuitive visualization methods are needed to support user cognition and leverage interaction technologies [19].

3.2 Related Work

Numerous approaches have been proposed to enhance the visualization of dynamic and multivariate networks. This section presents three techniques that serve as references for the present work.

Linhares et al. [20] proposed Community-based Node Ordering (CNO), a technique for organizing nodes according to community structure in order to reduce edge visual clutter in dynamic networks. The method involves three steps: (i) community detection, (ii) reordering of communities to minimize edge crossings, and (iii) reordering of nodes within communities to highlight local trends. The process can be repeated iteratively until no further subdivision is needed.

Implemented in the DyNetVis tool [21], CNO was applied to a Twitter dataset containing more than 50,000 nodes. Compared to chronological ordering, CNO reduced edge overlap by up to 98.64% through the use of filters and hierarchical community detection, significantly improving visual clarity.

Although CNO is effective for visual simplification and the analysis of large-scale temporal networks, its application to very large networks faces limitations, particularly in maintaining a balance between visual clarity and the preservation of relevant information. Moreover, it does not handle explicit node attributes.

Wang et al. [10] developed Multi-NetVis, a visual analysis platform for multivariate networks using combined 2D, 2.5D, and 3D *layouts*. The system supports force-based and community-based layouts, layered attribute visualizations, and matrix-based views. Nodes and edges are color-coded and spatially grouped by attributes.

The approach was demonstrated using brain connectivity data from Alzheimer's patients and healthy individuals. The layered visualizations revealed differences in connectivity and centrality, allowing users to identify abnormal patterns and weakly connected regions in the Alzheimer's group.

Although powerful for detailed analyses, Multi-NetVis presents lower scalability for large networks, owing to the complexity of multidimensional panels and the spatial constraints of 3D navigation.

Vehlow et al. [9] introduced a matrix-based visualization approach for hierarchical group structures in dynamic graphs. Networks are displayed as a sequence of adjacency matrices, with nested borders representing group hierarchies. Curved Bézier connectors illustrate transitions over time, highlighting structural changes.

The technique was applied to a longitudinal dataset of international football matches. Three hierarchical structures were compared: local annual clusterings, clusterings stabilized over time, and static geographic clusterings. The visual encodings revealed consistent groupings, such as Oceania teams, and temporal events, such as qualification phases for global tournaments.

Although the method effectively conveys temporal and hierarchical patterns, it becomes challenging with very large networks, owing to pixel density constraints and visual complexity.

Fuchs et al. [22] extended the BioFabric system, originally designed for dense networks, to support the visualization of multivariate data. In this *layout*, nodes are displayed as horizontal lines and edges as vertical lines on a grid. The authors introduced visual encodings for node and edge attributes using variations in thickness, curvature, color, and bar charts. Their system also supports redundant encoding, combining multiple visual channels to reinforce attribute interpretation without sacrificing topological clarity. They analyzed a network of fictional characters, in which attributes such as age, ranking, and screen time were encoded through dash patterns and stacked bars. Although effective for conveying attribute-rich data, the method may suffer from visual overlap and reduced legibility in highly multivariate or dense networks.

Chang et al. [23] proposed DGVis, a visual analysis system for dynamic networks featuring subtle structural changes over time. The system employs hierarchical temporal aggregation to create variable-length time slices, which are projected into a 2D space using t-SNE. Structurally similar snapshots appear closer together, with line color and width encoding recency and transition. DGVis also provides detailed node-edge visualizations, spatial interaction maps, and temporally aligned line charts for multiple metrics such as speed, degree, and average distance.

These studies demonstrate different ways of visualizing dynamic networks. However, most do not fully incorporate node attributes into the layout computation. This work aims to bridge that gap by proposing attribute-aware layout strategies that enhance both the semantic interpretation and structural analysis of dynamic multivariate networks.

4. Methodology

This work proposes an extension of the Recurrent Neighbors (RN) strategy [8] to incorporate node attributes into the analysis. Our method integrates topological and semantic node properties to enhance the interpretability of dynamic multivariate networks.

4.1 Recurrent Neighbors (RN)

The *Recurrent Neighbors* (RN) technique was proposed to highlight frequent interaction patterns in temporal networks, centralizing the most active nodes in the temporal *layout* while minimizing the length of vertical edges. This technique aims to reduce edge overlap and visual clutter by spatially positioning nodes with recurrent interactions over time closer to one another. The process begins by identifying the node with the highest cumulative degree or temporal activity, which is placed at the central row of the *layout*. Iteratively, nodes with the greatest number of recurrent connections to the reference node are allocated to adjacent rows (above and below), prioritizing the frequency of temporal interactions. This procedure continues by selecting, at each step, a new node with strong recurrent connectivity to the last positioned node, until all nodes are arranged. Should any unallocated nodes remain — that is, nodes with no direct connections to any already-positioned node — the algorithm inserts them alternately at the beginning or end of the sequence, based on the degree of connection with the nodes located at each extremity. This ensures that all nodes are included in the final ordering [8].

4.2 Attribute-based Recurrent Neighbors (ARN)

Our proposal generalizes this strategy by combining node degree with normalized node attributes.

The Attribute-based Recurrent Neighbors (ARN) method proposed in this work extends the traditional Recurrent Neighbors (RN) approach by incorporating intrinsic node characteristics into the ordering process, in addition to degree, which is the primary parameter of the traditional RN approach. In ARN, degree is treated as an attribute subject to weighting and combined with other normalized node attributes, allowing this information to influence the *layout* construction. To support multiple analytical perspectives from the same dataset, users may assign custom weights to each attribute, defining the relative importance of each node characteristic in the ordering.

The *Sequence View* visualization offers interactive functionalities that broaden its applicability, such as dynamic node reordering [16]. In this context, the method proposed in this work defines node positioning in the temporal *layout* by bringing closer those nodes that not only exhibit greater interactivity but also share compatible characteristics. Algorithm 1 presents the proposed method, whose steps are discussed below. The input network is defined as $R = (V, E)$, where V is the set of nodes and E is the set of edges. The node attribute matrix $A \in \mathbb{R}^{|V| \times d}$ contains $|V|$ rows (nodes) and d columns (attribute dimensions). The user-defined weight vector is denoted by $W \in \mathbb{R}^d$, and $w_g \in \mathbb{R}$ represents the weight assigned to the degree $\deg(v)$ in the initial scoring. The "relative degree" between a candidate node $v \in V$ and a reference node $u \in V$ is the connection strength $e_{vu} \in E$, optionally weighted by edge or adjacency values.

Algorithm 1: Node ordering using the Attribute-based Recurrent Neighbors (ARN) strategy.

Input : Network $R = (V, E)$, attribute matrix $A \in \mathbb{R}^{|V| \times d}$, weight vector $W \in \mathbb{R}^d$, degree weight $w_g \in \mathbb{R}$
Output : Ordered list of nodes *finalList*

foreach *node* $n \in V$ **do**
  $score[n] \leftarrow w_g \cdot degree(n) + \sum_{i=1}^{d} W[i] \cdot A[n][i]$;
initialList $\leftarrow$ nodes sorted in descending order of $score[n]$;
finalList $\leftarrow$ [*initialList*[0]];
$first \leftarrow initialList[0]$, $last \leftarrow initialList[0]$;
Remove *initialList*[0];
$currentExt \leftarrow first$;
while *initialList* $\neq$ [] **do**
  foreach *node* $n_1 \in initialList$ **do**
    Compute $scoreRel(n_1, currentExt)$;
  chosenCandidate $\leftarrow$ node with highest *scoreRel*;
  if $currentExt = first$ **then**
    Insert *chosenCandidate* at the beginning of *finalList*;
    $first \leftarrow chosenCandidate$;
  else
    Insert *chosenCandidate* at the end of *finalList*;
    $last \leftarrow chosenCandidate$;
  Remove *chosenCandidate* from *initialList*;
  if $currentExt = first$ **then**
    $currentExt \leftarrow last$;
  else
    $currentExt \leftarrow first$;
return *finalList*

The proposed algorithm begins by computing an initial score for each node $n \in R$, combining its degree — which represents the total number of connections initiated or received — weighted by w_g, with the weighted sum of its attributes $A[n][i]$, according to the weights defined in the vector W. Nodes are then sorted in descending order based on these scores, forming the `initialList`.

The node with the highest score is selected as the starting point and added to the `finalList`, initially acting as both the `first` and `last` element in the sequence. The variable `currentExt` is used to track which end of the list should be used for comparison with the remaining candidates, alternating between `first` and `last` at each iteration.

During the main loop, the algorithm recalculates, for each remaining candidate, a relative score denoted by (scoreRel(c, `currentExt`)), which combines the candidate's connectivity with the current endpoint (`currentExt`) and a weighted sum of its attributes. Next, the candidate with the highest (scoreRel) value is selected and inserted at the appropriate end of the final list (`finalList`): at the beginning if `currentExt = first`, or at the end if `currentExt = last`.

The *scoreRel* of a candidate c with respect to an endpoint e is

computed as shown in Equation (1).

$$\text{scoreRel}(c,e) = \frac{\text{connectionScore}(c,e) - g_{\min}}{g_{\max} - g_{\min}} + \sum_{i=1}^{d} W[i] \cdot A[c][i] \quad (1)$$

The relative score between a candidate node c and a list endpoint e, denoted as $\text{scoreRel}(c,e)$, is computed by combining two components: the normalized number of edges between c and e computed by the *connectionScore* function, and the weighted sum of c's attributes. Normalization is based on the minimum and maximum number of edges observed among all candidates, ensuring that the connectivity component lies within the range $[0,1]$. This value is then added to the attribute-based score, enabling the selection of candidates that are simultaneously topologically close to the current endpoint and similar in terms of their attributes.

After insertion, the selected candidate is removed from the `initialList`, the appropriate endpoint is updated, and the value of `ext` is toggled for the next iteration. This process continues until all nodes have been ordered. Finally, the algorithm returns the `finalList`, which represents a node ordering that balances the initial attribute-based score with progressive relative connectivity as the sequence is built.

To illustrate the proposed algorithm, Figure 1 presents an application on a hypothetical network representing social interactions over time among users of a social platform. In this network, each person is represented by a node labeled as "Person_X," and the connections between nodes indicate social interactions such as conversations, meetings, or collaborations. For each individual, the considered attributes are Age (represented by shades of green), Education Level (orange), and Income (shades of blue) in the visualization. The underlying hypothesis is that Income exerts an influence on connection formation as significant as Age and Education Level.

The analysis of the ARN-based network visualization highlights spatial segregation. In Figures 1a, b, and c, nodes are colored by Age, Income, and Education Level, respectively. The first two rows display degree-based and RN-based orderings, while the third row shows the ARN ordering, alternating weights assigned to the attributes. When ordered by degree, nodes appear scattered without a clear organization by attributes. In contrast, the traditional Recurrent Neighbors ordering, illustrated in Figures 1d, e, and f, suggests only a subtle proximity among nodes with similar tones. A more distinct gradient organization emerges in Figures 1g, h, and i, which incorporate attributes into the ordering with weights [Degree=1, Age=0.5, Income=0.3, Education Level=0.5]. Nodes with stronger shades of green (Age), blue (Income), and orange (Education Level) tend to cluster near the center of the layout, forming cohesive groupings. The higher cohesion observed for Income and Education Level compared to Age suggests that these attributes structure the network more strongly. It is particularly noteworthy that for Income, this centrality effect emerges even when the attribute weight is relatively low, indicating that its qualitative influence on social configuration may be underestimated by the initial weights.

5. Connectivity Mapping by Color Encoding

The use of color in this work primarily aims to support the interpretation of possible relationships between node attributes and the connections they establish within the network, facilitating the identification of structural patterns associated with those attributes. To optimize this interpretation, the color mapping is adapted according to the nature of the attribute: for numerical values, a continuous color gradient is applied, with values rescaled between the minimum and maximum to match the gradient range; for categorical attributes, each distinct value receives a unique and contrasting color, ensuring easy distinction between categories. Nodes with missing or invalid attribute data are displayed in gray, signaling the absence of available information without interfering with the overall network legibility.

6. Experiments

This section presents the application of the proposed method to two datasets describing social interactions among *Papio papio*, collected at the CNRS Primatology Centre in Rousset-sur-Arc, France [11].

6.1 Experimental Setup

Computational experiments were conducted using two versions of the dataset provided by the CNRS Primatology Centre, under the hypothesis that individual attributes — such as age, gender, and kinship — would influence the group's social dynamics over time.

The first dataset — referred to here as the Observation Dataset — was obtained through direct observation, recording 3,040 behavioral interactions involving 20 individuals over a 20-day period in 2019. Each entry represents a directed interaction between two individuals, annotated with timestamps and node attributes such as age and gender. The second dataset — referred to here as the Sensor Dataset — comprises 54,852 proximity events detected by wearable sensors among a subset of 13 juvenile and adult individuals. Each event was recorded when two sensors detected face-to-face proximity within 1.5 meters, with a temporal resolution of 20 seconds [11]. Both datasets were filtered to include only interactions with complete node attribute information. Additional kinship data for some baboons were obtained directly from the French Primatology Centre (CNRS), located in Rousset-sur-Arc, where the primates are housed.

Data preprocessing involved rescaling continuous attributes to the range [0, 1] using the Min-Max technique, in order to standardize scales and enable consistent comparisons [24]. Additionally, for categorical attributes, a binary similarity strategy was adopted in two distinct stages: (i) in the initial scoring, each categorical attribute was evaluated against the mode of its values, assigning 1 if the node had the modal value and 0 otherwise; and (ii) in the interleaving stage, the comparison was performed directly between the candidate node

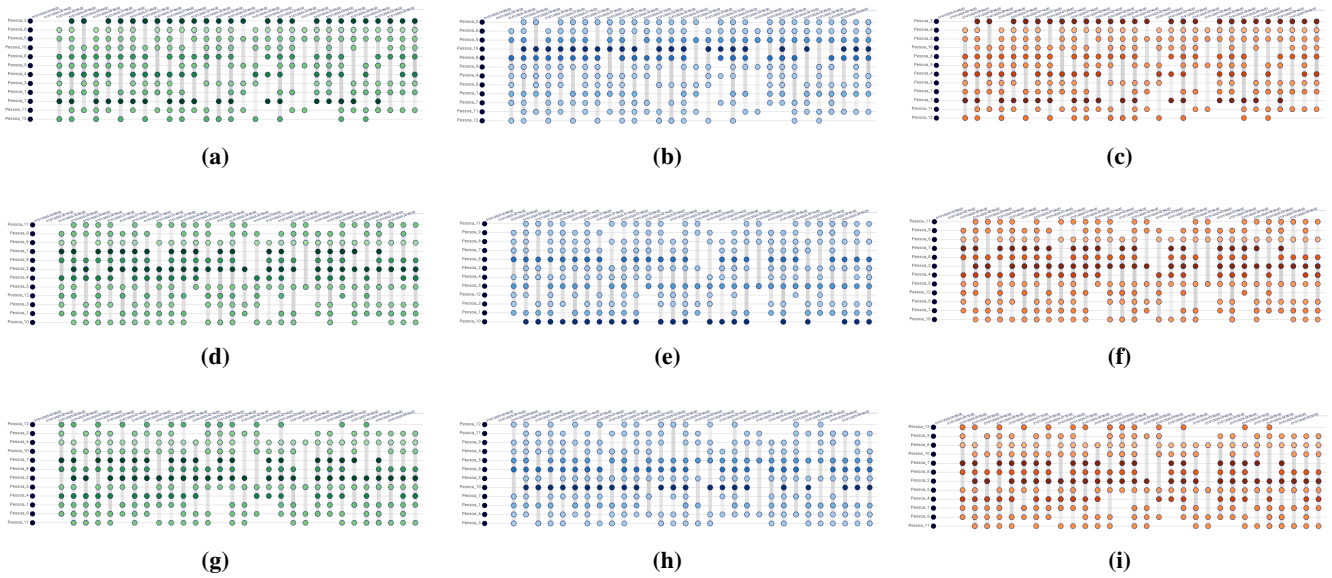


Figure 1. ARN: influence of attributes on node ordering. In the first column, nodes are colored by Age; in the second, by Income; and in the third, by Education Level. The first two rows show nodes ordered by Degree and RN, respectively, while in the third row, nodes are ordered by ARN with weights [Degree=1, Age=0.5, Income=0.3, Education Level=0.5].

and the reference node, receiving 1 if both shared the same categorical value and 0 otherwise. This approach preserves the original attributes for comparison, employing the mode during the initial scoring and direct equality in the relative stage, thereby maintaining the natural semantics of the categories. Similar strategies are widely described in data mining and categorical attribute clustering techniques [25, 26, 27].

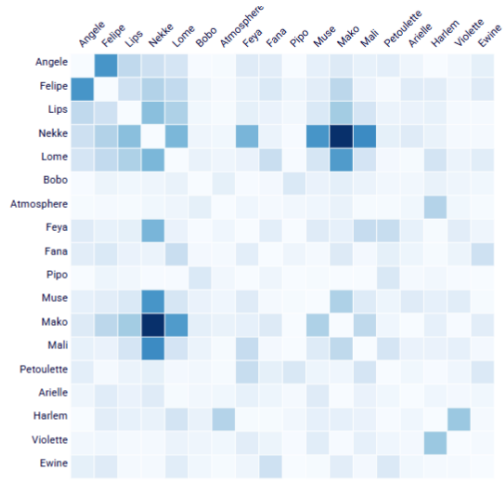


Figure 2. Adjacency matrix — representing bidirectional interactions between nodes in a network. The number of connections between individuals is mapped by the cell color intensity. The less intense the shade of blue, the greater the number of connections, and vice versa.

6.2 Observation Dataset Results

The analysis of the *Observation Dataset* revealed significant patterns in the social interactions of the baboons, as demonstrated by the following visualizations. Figure 2 presents the adjacency matrix of the complete network, illustrating the distribution of connections among individuals.

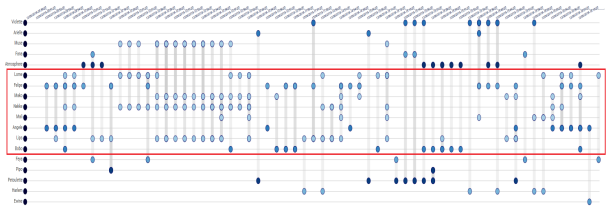
From Figure 2, distinct connectivity patterns among individuals can be observed. Stronger connections, indicated by dark shades of blue, highlight pairs such as Nekke and Mako, as well as Mako and Lomé, suggesting frequent social bonds that are relevant to the network structure. Intermediate-intensity connections, such as between Petoulette and Feya or Harlem and Atmosphere, although less frequent, still contribute to network cohesion. Lighter shades, on the other hand, indicate sporadic interactions between individuals such as Ewine and Mali or Lips and Violette. These patterns suggest that the network is sustained by a combination of strong

central connections and weaker relationships, with certain individuals playing structurally important roles in this social network.

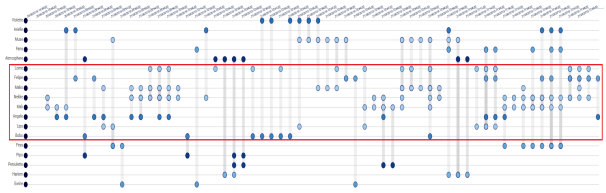
To examine the temporal evolution of interactions, three representative intervals were defined — referred to as Intervals A, corresponding to the beginning, middle, and end of the observed period:

1. from 09:50 on 13.06.2019 to 16:13 on the same day;
2. from 15:45 on 20.06.2019 to 11:49 on 21.06.2019;
3. from 15:07 on 08.07.2019 to 13:10 on 09.07.2019.

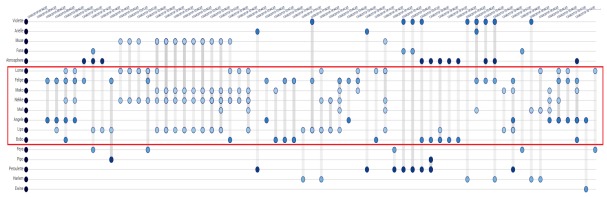
These intervals were used to construct the *Sequence View* (SV) and TAM *layouts*. Figures 3a, 3b and 3c present the *Sequence View* with Recurrent Neighbors ordering (using only degree) and node coloring based on the age of the primates.



(a)



(b)

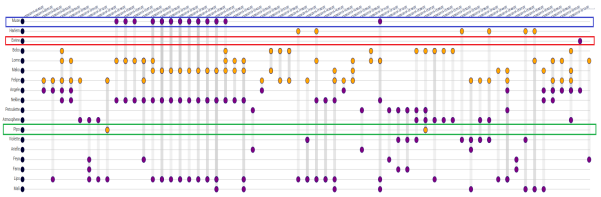


(c)

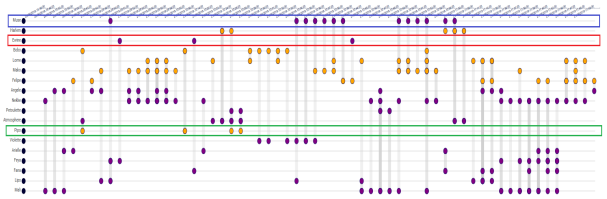
Figure 3. SV – Nodes ordered by recurrent neighbors considering only degree and colored according to the age of the primates. Figures a, b, and c represent the first, second, and third observed in Intervals A, respectively.

The visualizations indicate that younger individuals, represented by lighter-colored circles, tend to occupy the central regions of the *layout* and maintain a greater number of connections. This pattern is consistent across the three intervals, suggesting that youth is associated with high sociability within the group.

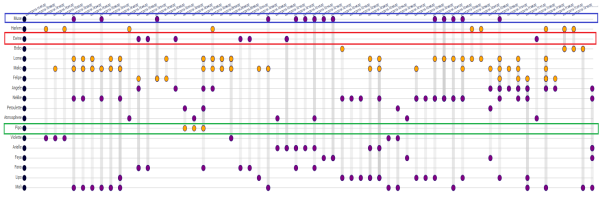
Figure 4 presents a new set of visualizations generated by ordering nodes using ARN, with the weight configuration [Degree = 1, Gender = 0, Age = 1]. In this visualization, nodes are colored according to the gender of the individuals. Each image represents one of the three temporal segments defined in Intervals A (a, b, and c), as described previously.



(a)



(b)



(c)

Figure 4. SV - Recurrent neighbor ordering with weights configured as [Degree=1, Gender=0, Age=1], coloring the nodes by gender. The three time intervals are divided among a, b, and c as defined in Intervals A.

From Figures 4a, 4b, and 4c, it can be observed that Ewine, a 9-year-old female baboon, appears to maintain a frequent interaction pattern with individuals of the opposite gender and from different age groups, as reflected by her positions among the orange nodes. When examining the connections and node colors in the *layout*, *Papio papio* seem to establish mixed interactions, maintaining a balanced communication pattern between genders. Figure 4 also highlights individuals who interact across different genders and age groups, such as Muse, a 2-year-old female, and Pipo, an older male. This pattern suggests that these primates may play connector or intermediary roles in the social network. In addition, Lomé and Mako, two juvenile males, stand out by presenting multiple connections between each other, as also emphasized by the adjacency matrix. These observations illustrate the social dynamics and structural relationships present in the network.

To investigate the temporal dynamics of connections more thoroughly, the TAM was employed, as presented in Figure 5. Nodes were ordered using the ARN method, with attribute

weights configured as [Degree = 0.5, Gender = 0, Age = 1].

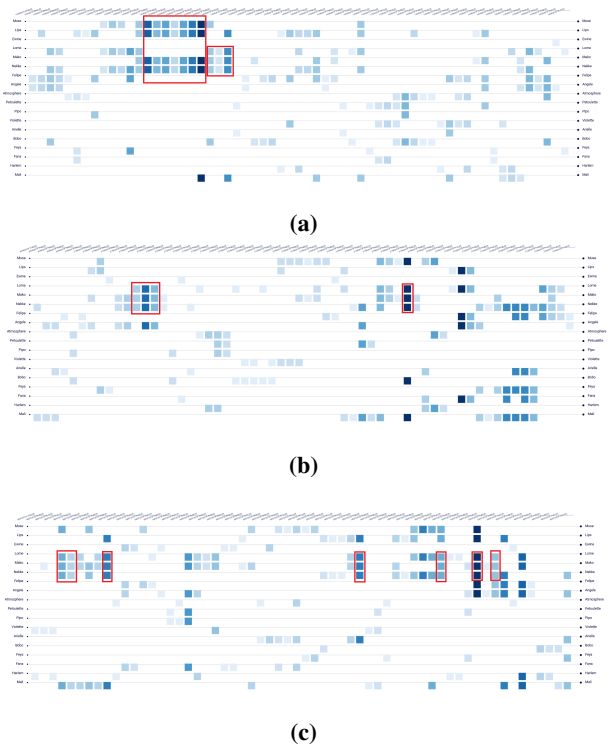


Figure 5. TAM - Recurrent neighbor ordering with weights configured as [Degree=0.5, Gender=0, Age=1] in the TAM *layout*. As per Interval A, the subfigures a, b, and c correspond to three temporal divisions.

In Figure 5a, the proximity between nodes Mako and Nekke, as well as between Lips and Muse, in the TAM *layout* highlights similarities in their static attributes (age and gender) and in their relative degree of connectivity—a dynamic attribute that considers the local connections of the network and directly influences node ordering. This pattern is observed on 13/06/2019, between 10:28 and 10:36, and again between 10:36 and 10:38, in the close positioning of Lomé, Mako, and Nekke. In Figure 5b, the concentration of these same individuals between 09:53 and 09:56, and at 10:51 on 21/06/2019, reinforces this consistency. Similarly, Figure 5c shows them in close proximity in the *layout* at 15:21, 15:22, and 15:41 on 08/07/2019, as well as at 10:29, 10:41, 10:58, and 10:59 on 09/07/2019. These results suggest that, at this stage of life, age plays a relevant role in the formation of connections, as reflected in the close positioning of these nodes in the *layout*. In the analyzed social context, this pattern may indicate that juveniles of the same age group share more frequent interactions and stronger bonds, suggesting that age brings individuals together regardless of gender.

Finally, Figure 6 presents an ordering that prioritizes gender ([Degree=0.5, Gender=1, Age=0]), enabling a direct comparison of the impact of age and gender on cluster formation.

In the configuration with weights [Degree=1; Gender=0.5; Age=0.5], the miniature of the *Activity Map* at Figure 6a reveals a slight concentration of nodes in the central region. This result suggests that, by assigning greater weight to connectivity, degree regains a predominant role in the global organization. Nevertheless, the inclusion of age and gender in the weighting introduces local adjustments, softening the formation of the central core and allowing greater diversity of groupings in the *layout*. When comparing Figures 6b and 6c in the *Sequence View*, it becomes evident that the network core is not exclusively shaped by either age or gender. Age-based visualizations highlight some groupings, particularly among younger individuals, while gender-based views reveal no consistent separation between males and females, who remain mixed in the central region. These results suggest that age may foster proximity in specific contexts, but both attributes act only partially and do not solely define the social structure. Overall, the layouts indicate that age and gender contribute to the visual organization of the *Papio papio* social network but are not dominant factors on their own; degree continues to play a central role in the global arrangement. Local age-based clusters—especially among younger individuals—coexist with a mixed gender distribution in the core, a pattern consistent across the Sequence View, adjacency matrix, and TAM miniatures. Thus, while age can favor interaction patterns, its effect is partial and dependent on connectivity and parameter settings, reinforcing that causal conclusions about

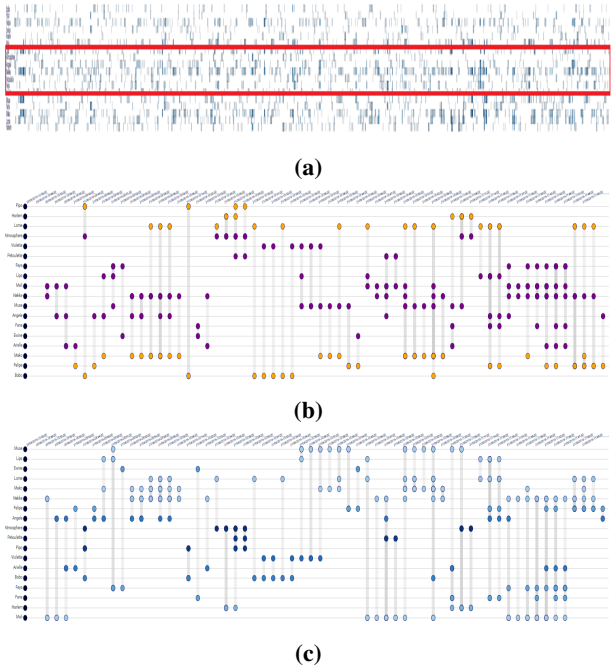


Figure 6. RN ordering with weights configured as [Degree=1, Gender=0.5, Age=0.5] in the mini TAM *layouts* (a), SV coloring the nodes by gender and RN ordering with weights configured as [Degree=0.5, Gender=1, Age=0] in (b), and ordered by RN [Degree=0.5, Gender=0, Age=1] and colored by age (c) in selected network segments.

attribute influence require complementary statistical analyzes.

6.3 Sensor Dataset Results

The adjacency matrix formed from the sensor-collected data revealed several connectivity patterns among the baboons (Figure 7). In this case, there are no juveniles in the dataset. Within this context, the pairs Ewine and Fana, Ewine and Angele, as well as Angele and Felipe stand out — all younger individuals of similar ages — confirming the trend identified in the first network, that younger baboons tend to interact more. Arielle and Bobo, however, despite belonging to a middle-age group, continue to show low activity in the network, as also observed in the observation dataset.

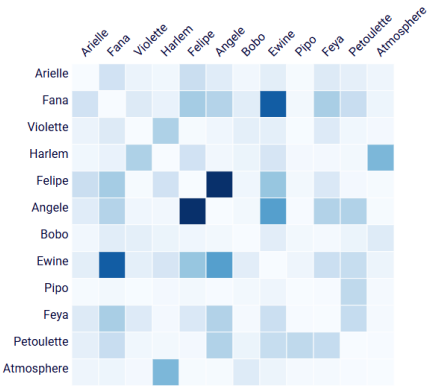


Figure 7. Adjacency matrix colored according to node degree. The number of connections between individuals is mapped by the cell color intensity, such that the less intense the blue, the greater the number of connections.

Older primates, such as Atmosphere, Petoulette, and Pipo, maintained a lower level of activity. Among them, Atmosphere showed more interactions with Harlem, aged 6, while Petoulette connected more with Angele, Ewine, Feya, and Pipo. Female *Papio papio* are dispersers in the social structure of the species [28]. Pipo, on the other hand, maintained closer contact with Petoulette — possibly a strategic bond, consistent with [29], which suggests that older primates, owing to their accumulated experience and philopatric nature, tend to value previously established strong relationships rather than seeking extensive connections.

To generate the visualizations for the Sequence View *layout*, three representative intervals from the beginning, middle, and end of the network were selected, referred to as Intervals B:

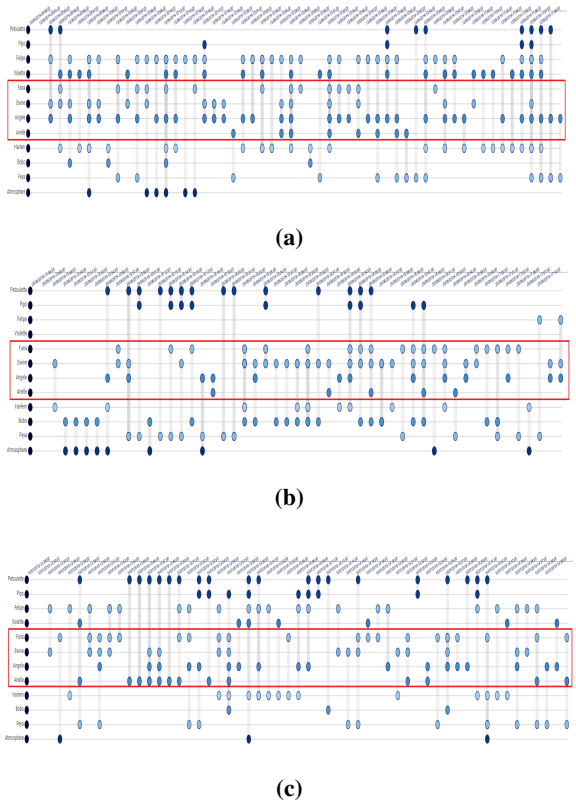
1. 13.06.2019 from 09:50 to 11:08;
2. 20.06.2019 from 15:45 to 17:14;
3. 10.07.2019 from 13:28 to 14:39.

For the Temporal Activity Map (TAM), which requires greater spacing between temporal instants, three broader segments were defined to capture the beginning, middle, and end of the network timeline, referred to as Intervals C:

1. 13.06.2019 from 06:32 to 07:37;
2. 02.07.2019 from 18:43 to 20:09;
3. 10.07.2019 from 06:18 to 07:37.

These intervals were selected to ensure representative samples across the full temporal extent of the dataset.

Figure 8 presents the *Sequence View* (SV) *layout* applied to the sensor-collected dataset, divided into three representative temporal intervals from the beginning, middle, and end of the network, as defined in Intervals B.



(a)

(b)

(c)

Figure 8. SV – Ordering by recurrent neighbors, with node coloring based on age. The intervals in a, b, and c represent samples from the beginning, middle, and end of the network. Apart from degree, no other attribute was considered in this ordering.

In this visualization, a predominance of lighter-colored nodes is observed in the central region of the *layout* across all three intervals 8a, 8b and 8c. However, compared to the same *layout* in the observation network, a greater presence of intermediate tones is noted in this area. The younger, more active baboons stand out across the analyzed intervals, while the emergence of intermediate tones suggests that, in the absence of juveniles, middle-aged individuals also play a significant role in the network's dynamics. Arielle, for example, appears among the central nodes, despite showing low activity in the adjacency matrix.

Figure 9 is divided into three parts: Fig. 9a, which shows the TAM minimap ordered by Recurrent Neighbors with

weights configured as [Degree = 0.5, Gender = 1, Age = 0], providing an overview of network activity; Fig. 9b, which presents the SV under the same ordering with nodes colored by age; and Fig. 9c, with nodes colored by gender, facilitating the perception of these characteristics.

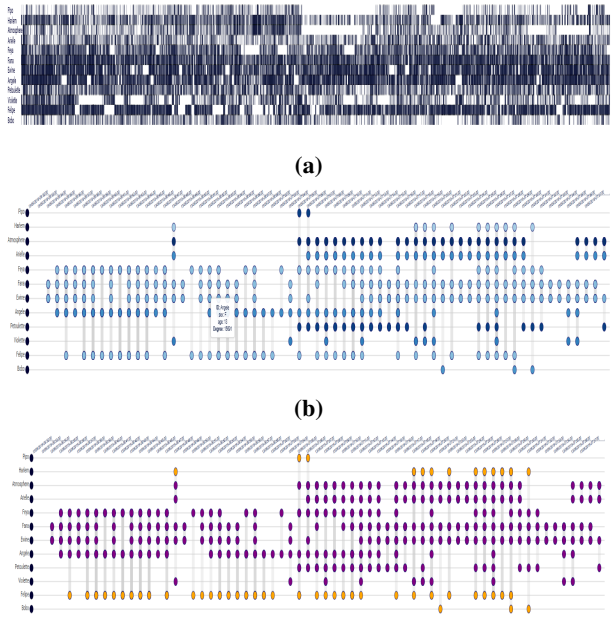


Figure 9. RN ordering with weights configured as [Degree=0.5, Gender=1, Age=0] in the mini TAM *layouts* (a), SV coloring the nodes by age (b), and by gender (c) in selected network segments.

Figure 9a highlights the concentration of network activity in the central region of the *layout*. Comparing the views in Figures 9b and 9c in the SV, it can be observed that the network core, under this ordering, is largely composed of younger baboons, even though gender was configured as the attribute with the highest influence on node positioning. This result is consistent with the trend also identified in the observation network, where individuals of both genders occupy central positions in the *layout*. The combination of these layouts suggests that age plays a relevant role in the social organization of *Papio papio*, bringing younger individuals closer to central positions, while gender and connectivity also contribute to the global configuration.

The SV *layout* shown in Figure 10 displays the result of applying the Attribute-based Recurrent Neighbors method, using the weight configuration [Degree = 1, Gender = 0, Age = 1], and coloring nodes according to the gender of the primates.

The pattern observed in Figures 10a and 10c, and more clearly in Figure 10b, suggests a predominance of female individuals in the central positions of the network. However, Feya and Arielle maintain frequent interactions with male baboons, while Felipe and Bobo follow a similar pattern by connecting with females.

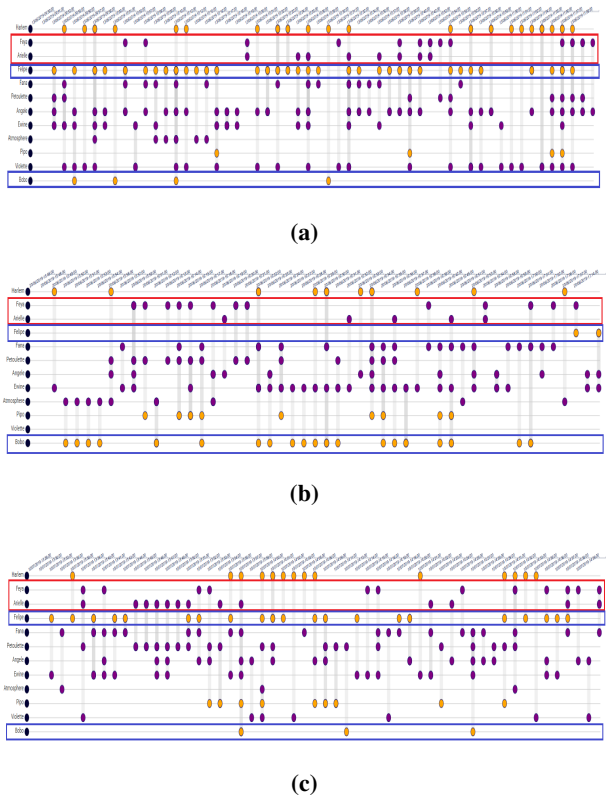


Figure 10. Sequence View visualization with nodes ordered by recurrent neighbors, using weights [Degree = 1, Gender = 0, Age = 1], and colored according to gender. The intervals a, b, and c represent samples from the initial, middle, and final portions of the network, as defined in Intervals B.

In this context, female individuals tend to occupy central positions in the network, while cross-gender interactions remain frequent, indicating that gender alone does not define the social structure. Instead, the observed patterns suggest a balance in which gender influences centrality, but connection dynamics are shaped by interactions across both sexes.

In light of this, investigating the kinship relationships among the baboons contributes to deepening the analysis. Figure 11 illustrates these relationships among three group members at different moments within Interval C, with nodes ordered by Recurrent Neighbors, disregarding the influence of attributes.

Figures 11a, 11b, and 11c present three network segments where the proximity between Petoulette and her offspring Felipe (highlighted in purple) and Angele (in orange) in the TAM layout reflects similarities in attributes and local connectivity patterns considered in the ordering. The results indicate that the relationship between the mother and her now-adult offspring remains relevant. Felipe, 8 years old, was positioned closer to his 19-year-old mother Petoulette than to his 13-year-old sister Angele. This observation suggests that, in this case, kinship exerts greater influence on the relative positioning

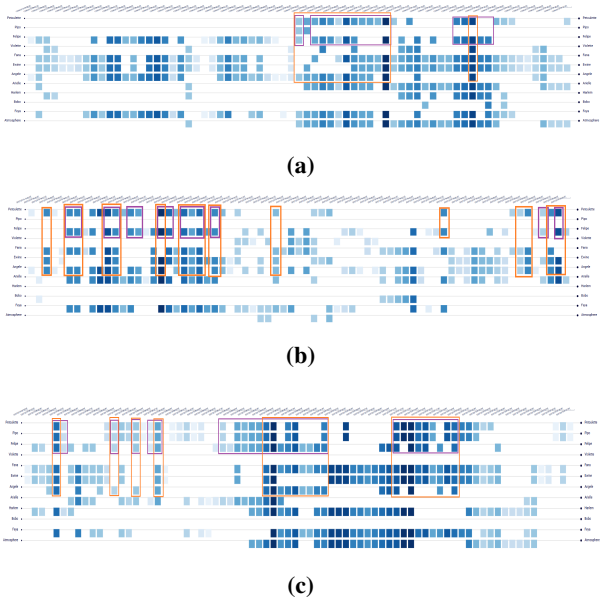


Figure 11. TAM — Recurrent Neighbors ordering without attribute influence, highlighting the relationship between mother Petoulette and her offspring Felipe (purple) and Angele (orange) across three distinct time intervals. Node color indicates connectivity at each temporal instant.

of these nodes in the *layout* than age, pointing to the need for further investigation of this pattern in the analyzed social context.

6.4 Visual Complexity

In the SV *layout*, connections between nodes are represented by vertical lines, with edge overlap being the primary factor contributing to visual complexity, which may hinder the perception of patterns in the network [8]. Figure 12 illustrates how overlaps occur under different node orderings.

Figure 12 highlights in red the connections that occurred on 13/06/2019 at 09:56:00. In the original ordering, 5 edges were overlapping. The number of overlaps observed in Figure 12b, where ordering was by degree, was 3. In Figure 12c, with RN-based ordering, the total was 5. In Figure 12d, using RN with attributes configured as [Degree = 1, Gender = 0.5, Age = 0], the number of overlaps was 3. In Figure 12e, where attribute weights were [Degree = 0.8, Gender = 0.3, Age = 1], the total number of observed overlaps was 6.

Visual complexity was quantified by an overlap counter, as described by 20, which employs: (i) per-instant counting, detecting vertical intersections between edges; and (ii) average overlap, obtained by dividing the sum of intersections by the number of time intervals. Algorithm 2 details the procedure.

Algorithm 2 iterates over all available temporal instants and, for each interval, extracts the associated edges. For each edge, the vertical interval is then computed based on the positions of the source and target nodes in the current ordering. By comparing all possible pairs of distinct intervals,

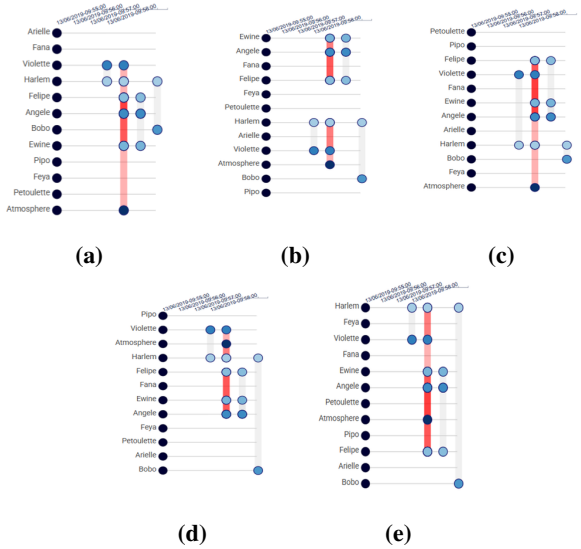


Figure 12. Overlaps in the SV *layout*: (a) original ordering; (b) degree; (c) RN; (d) RN [Degree=1, Gender=0.5, Age=0]; (e) RN [Degree=0.8, Gender=0.3, Age=1]. Red edges represent connections on 13/06/2019 at 09:56:00.

an overlap is detected whenever two intervals share a portion of the same vertical region — that is, when an intersection between them exists. Overlaps are counted only when the intersection exceeds a configurable threshold (in this case, **Threshold = 1**). Finally, the average number of overlaps is computed by dividing the total overlaps by the number of evaluated time intervals. This metric provides an estimate of the visual complexity caused by edge overlaps, directly impacting the legibility of the visualization.

The average number of overlaps detected in the *layouts* generated in this study was computed for different ordering methods and attribute combinations, as shown in Table 1.

Table 1. Edge overlap computation in the Sequence View *layout* to evaluate visual complexity. — D: Degree, G: Gender, A: Age. Green bars indicate reduction; red bars indicate increase relative to the original ordering.

Dataset	Ordering Strategy	Avg.	Variation (%)
Obs.	Original	0.77	0.00%
	Degree	0.72	-6.49%
	RN	0.73	-5.19%
	ARN (D=1, G=0.8, A=0.5)	0.76	+2.60%
	ARN (D=1, G=0.5, A=0.7)	0.79	-2.60%
	ARN (D=1, A=1)	0.74	-3.90%
	ARN (D=0.2, G=0.6)	0.71	-7.79%
Sens.	Original	1.02	0.00%
	Degree	0.93	-8.82%
	RN	1.05	+2.94%
	ARN (D=1, A=1)	1.11	+8.82%
	ARN (D=1, G=0.5, A=0.5)	0.94	-7.84%
	ARN (D=0.2, G=0.7, A=1)	1.02	0.00%
	ARN (D=1, G=1)	0.97	-4.90%

According to the results in Table 1, degree-based ordering consistently reduced overlaps in both datasets (–8.82% in Sensors and –6.49% in Observations), slightly improving readability. By contrast, ARN configurations showed more

Algorithm 2: *Average Visual Overlap Computation in SV*

Input : Temporal network with edge sets A_t for each instant $t \in T$
Output : Average number of visual overlaps between edges

Step 1: Initialization;
$overlap \leftarrow 0$;
Step 2: Per-temporal-instant processing;
foreach $t \in T$ **do**
  $edges_t \leftarrow$ getEdges(t);
  $intervals \leftarrow \emptyset$;
  Step 2.1: Vertical interval construction;
  foreach $a \in edges_t$ **do**
    $origin \leftarrow$ getVerticalPosition($a.origin$);
    $target \leftarrow$ getVerticalPosition($a.target$);
    $intervals[a] \leftarrow$ list of nodes sorted vertically between $a.origin$ and $a.target$, inclusive;
  Step 2.2: Overlap verification;
  foreach *pair* (i, j) *of intervals in intervals* **do**
    $intersection \leftarrow$ computeIntersection(i, j) ; `// Number of overlapping nodes`
    if $intersection > THRESHOLD$ **then**
      $overlap \leftarrow overlap + 1$;
Step 3: Final average computation;
$averageOverlap \leftarrow \frac{overlap}{|T|}$;
return $averageOverlap$;

variable effects: in Sensors, [Degree=1; Age=1] increased overlaps (+8.82%), while other combinations, such as [Degree=1; Gender=1], reduced them (–4.90%). In Observations, almost all ARN orderings yielded modest changes, with the largest reduction (–7.79%) for [Degree=0.2; Gender=0.6] and the highest average (+2.60%) for [Degree=1; Gender=0.8; Age=0.5]. These findings suggest that while degree acts as a stable baseline for reducing visual complexity, the impact of ARN orderings depends strongly on network structure and attribute composition.

Although the inclusion of attributes may increase overlaps in some cases, it enables the identification of social patterns not evident in connectivity-based orderings alone. For instance, when age received greater weight, individuals such as Atmosphere emerged as central; conversely, when age was excluded, Atmosphere's relevance diminished, showing that his position is more strongly linked to age than to degree or gender. In contrast, the prominence of the trio Angele, Ewine, and Felipe indicates consistent ties among younger baboons. The visualizations also suggest that age and gender modulate social bonds differently: females tend to cluster in central positions, whereas young males such as Harlem and Bobo appear more peripheral. Thus, even with occasional increases in overlaps, the flexibility of attribute weighting provides more informative insights into social dynamics, highlighting the role of node attributes in interpreting multivariate temporal networks.

7. Discussion

Experiments with the Attribute-based Recurrent Neighbors (ARN) technique, applied to the baboon social interaction dataset, revealed significant patterns that enhanced the understanding of network dynamics. Incorporating attributes such as degree, gender, and age into the node ordering process enabled the identification of relationships not captured by purely topological approaches, as well as the detection of social groups and hierarchies that would otherwise remain unnoticed. For instance, when nodes were colored by age or gender and arranged using the ARN technique, it became evident that individual attributes directly influenced the formation and frequency of interactions. Baboons of specific age groups or genders showed a greater tendency to form cohesive clusters and engage in more intense interactions, thereby revealing implicit social structures.

Moreover, the temporal analysis of connections showed that changes in node attributes—such as aging—were correlated with transformations in connection patterns, suggesting that these attributes can act as predictors of relational dynamics. Preserving the temporal order of interactions proved particularly important in the analysis of dynamic networks, as it allowed for the observation of the progression and reorganization of relationships over time—an aspect that would be lost in static analyses. Another relevant outcome was the improvement in the visual legibility of the networks. Attribute-driven ordering often contributed to reducing visual complexity, as reflected in the metrics presented in Table 1. This clearer organization facilitated the identification of connectivity patterns and improved data interpretation, even in the face of the inherent complexity of dynamic networks.

Finally, applying the technique across different datasets revealed important variations. In the observational dataset, the influence of attributes on group formation was more clearly detectable, likely due to the more relational and qualitative nature of the data. In contrast, in the sensor-based dataset, although the interactions were more circumstantial, the technique still highlighted behavioral patterns, suggesting its robustness even in scenarios with lower semantic quality.

8. Conclusion

This study presented a visualization strategy for Dynamic Multivariate Networks (DMNs) that adapts the Recurrent Neighbors technique to incorporate node attributes into the ordering process. By combining weighted ordering, flexible attribute configuration, and data-driven coloring, the approach enhanced both visual organization and analytical interpretation. Applied to observational and sensor-based datasets, the technique proved robust in revealing social groupings, hierarchies, and recurrent interaction patterns across different levels of semantic quality and temporal granularity.

The results demonstrated that attribute-driven ordering can improve interpretability even when edge overlap increases, suggesting that visual clarity is not always the primary crite-

rion in exploratory analysis. Age, gender, and degree influenced the formation of clusters and centrality in different ways, with some configurations emphasizing cohesive social structures more clearly than connectivity-based orderings alone. These findings highlight the importance of balancing structural, temporal, and semantic dimensions in dynamic network visualization, transforming layouts from mere representations of the network into analytical instruments.

Despite its contributions, the approach has limitations. Pairwise comparisons increase computational cost in large networks, and results are sensitive to the chosen temporal resolution and attribute quality. Future work should focus on automating weight calibration and extending applicability to networks with greater diversity of attributes. Overall, the proposed strategy strengthens the analytical power of network layouts by integrating connectivity, time, and semantics into a single visual space, paving the way for more nuanced explorations of complex multivariate networks.

Acknowledgments

This work was funded by the National Council for Scientific and Technological Development (CNPq) (402543/2021-1; 306436/2022-1). We are grateful to the Centre de Primatologie (CNRS, Rousset-sur-Arc) for kindly providing supplementary information about the dataset used in this study.

Author Contributions

Lorena Ferreira Marani was responsible for Investigation, Software, Data Curation, Result Analysis, and Original Draft Writing. Dr. José Gustavo de Souza Paiva and Dr. Bruno Augusto Nassif Travençolo contributed to Conceptualization, Supervision, and Manuscript Review.

References

[1] ALBERT, R.; BARABáSI, A.-L. Statistical mechanics of complex networks. *Reviews of Modern Physics*, American Physical Society (APS), v. 74, n. 1, p. 47–97, jan. 2002. ISSN 1539-0756. Disponível em: ⟨http://dx.doi.org/10.1103/revmodphys.74.47⟩.

[2] LEME, D. E. d. C. et al. Network analysis: A multivariate statistical approach for health science research. *Geriatrics, Gerontology and Aging*, Sociedade Brasileira de Geriatria e Gerontologia, v. 14, n. 1, p. 43–51, 2020. ISSN 2447-2123. Disponível em: ⟨http://dx.doi.org/10.5327/Z2447-212320201900073⟩.

[3] GARCíA-MEDINA, A.; C., J. B. H. Network analysis of multivariate transfer entropy of cryptocurrencies in times of turbulence. *Entropy*, MDPI AG, v. 22, n. 7, p. 760, jul. 2020. ISSN 1099-4300. Disponível em: ⟨http://dx.doi.org/10.3390/e22070760⟩.

[4] SONG, C. et al. Limits of predictability in human mobility. *Science*, v. 327, n. 5968, p. 1018–1021, 2010.

[5] HOLME, P.; SARAMäKI, J. Temporal networks. *Physics Reports*, Elsevier BV, v. 519, n. 3, p. 97–125, out. 2012. ISSN 0370-1573. Disponível em: ⟨http://dx.doi.org/10.1016/j.physrep.2012.03.001⟩.

[6] KALE, B.; SUN, M.; PAPKA, M. E. The state of the art in visualizing dynamic multivariate networks. *Computer Graphics Forum*, Wiley, v. 42, n. 3, p. 471–490, jun. 2023. ISSN 1467-8659. Disponível em: ⟨http://dx.doi.org/10.1111/cgf.14856⟩.

[7] MUNZNER, T. *Visualization Analysis and Design*. 1. ed. Boca Raton: AK Peters, 2014. 428 páginas. ISBN-10: 1466508914. ISBN 9781466508910.

[8] LINHARES, C. D. G. et al. Dynetvis: a system for visualization of dynamic networks. In: *Proceedings of the Symposium on Applied Computing*. ACM, 2017. p. 187–194. Disponível em: ⟨http://dx.doi.org/10.1145/3019612.3019686⟩.

[9] VEHLOW, C.; BECK, F.; WEISKOPF, D. Visualizing dynamic hierarchies in graph sequences. *IEEE transactions on visualization and computer graphics*, IEEE, v. 22, n. 10, p. 2343–2357, 2015.

[10] WANG, S. et al. Multi-netvis: Visual analytics for multivariate network. *Applied Sciences*, MDPI AG, v. 12, n. 17, p. 8405, ago. 2022. ISSN 2076-3417. Disponível em: ⟨http://dx.doi.org/10.3390/app12178405⟩.

[11] GELARDI, V. et al. Measuring social networks in primates: wearable sensors versus direct observations. *Proceedings of the Royal Society A: Mathematical, Physical and Engineering Sciences*, The Royal Society, v. 476, n. 2236, abr. 2020. ISSN 1471-2946. Disponível em: ⟨http://dx.doi.org/10.1098/rspa.2019.0737⟩.

[12] GULLSTRAND, J.; CLAIDIèRE, N.; FAGOT, J. Age effect in expert cognitive flexibility in guinea baboons (*Papio papio*). *Behavioural Brain Research*, Elsevier, v. 434, p. 114043, 2022. ISSN 0166-4328. Disponível em: ⟨https://www.sciencedirect.com/science/article/pii/S0166432822003114⟩.

[13] OKOE, M.; JIANU, R.; KOBOUROV, S. Node-link or adjacency matrices: Old question, new insights. *IEEE Transactions on Visualization and Computer Graphics*, Institute of Electrical and Electronics Engineers (IEEE), v. 25, n. 10, p. 2940–2952, out. 2019. ISSN 2160-9306. Disponível em: ⟨http://dx.doi.org/10.1109/TVCG.2018.2865940⟩.

[14] BACH, B.; PIETRIGA, E.; FEKETE, J.-D. Visualizing dynamic networks with matrix cubes. In: *Proceedings of the SIGCHI Conference on Human Factors in Computing Systems*. ACM, 2014. (CHI '14), p. 877–886. Disponível em: ⟨http://dx.doi.org/10.1145/2556288.2557010⟩.

[15] LINHARES, C. D. G. et al. A comparative analysis for visualizing the temporal evolution of contact networks: a user study. *Journal of Visualization*,

Springer Science and Business Media LLC, v. 24, n. 5, p. 1011–1031, jun. 2021. ISSN 1875-8975. Disponível em: ⟨http://dx.doi.org/10.1007/s12650-021-00759-x⟩.

[16] ELZEN, S. van den et al. Reordering massive sequence views: Enabling temporal and structural analysis of dynamic networks. In: *2013 IEEE Pacific Visualization Symposium (PacificVis)*. IEEE, 2013. p. 33–40. Disponível em: ⟨http://dx.doi.org/10.1109/PacificVis.2013.6596125⟩.

[17] SHNEIDERMAN, B. The eyes have it: A task by data type taxonomy for information visualizations. In: *Proceedings of the IEEE Symposium on Visual Languages*. [S.l.]: IEEE, 1996. p. 336–343.

[18] RODRIGUES, E. M. et al. Group-in-a-box layout for multi-faceted analysis of communities. In: *2011 IEEE Third Int'l Conference on Privacy, Security, Risk and Trust and 2011 IEEE Third Int'l Conference on Social Computing*. IEEE, 2011. p. 354–361. Disponível em: ⟨http://dx.doi.org/10.1109/PASSAT/SocialCom.2011.139⟩.

[19] BECK, F. et al. A taxonomy and survey of dynamic graph visualization. *Computer Graphics Forum*, Wiley, v. 36, n. 1, p. 133–159, jan. 2016. ISSN 1467-8659. Disponível em: ⟨http://dx.doi.org/10.1111/cgf.12791⟩.

[20] LINHARES, C. D. et al. A scalable node ordering strategy based on community structure for enhanced temporal network visualization. *Computers & Graphics*, Elsevier BV, v. 84, p. 185–198, nov. 2019. ISSN 0097-8493. Disponível em: ⟨http://dx.doi.org/10.1016/j.cag.2019.08.006⟩.

[21] LINHARES, C. D. G. et al. Dynetvis - an interactive software to visualize structure and epidemics on temporal networks. In: *2020 IEEE/ACM International Conference on Advances in Social Networks Analysis and Mining (ASONAM)*. IEEE, 2020. p. 933–936. Disponível em: ⟨http://dx.doi.org/10.1109/ASONAM49781.2020.9381304⟩.

[22] FUCHS, J. et al. Exploring the design space of biofabric visualization for multivariate network analysis. *Computer Graphics Forum*, Wiley, v. 43, n. 3, p. e15079, maio 2024. ISSN 1467-8659. Accessed: 2024-05-27. Disponível em: ⟨https://onlinelibrary.wiley.com/doi/abs/10.1111/cgf.15079⟩.

[23] CHANG, B. et al. Dgsvis: Visual analysis of hierarchical snapshots in dynamic graph. *arXiv preprint arXiv:2205.13220*, arXiv, abs/2205.13220, maio 2022. Accessed: 2024-05-30. Disponível em: ⟨https://arxiv.org/abs/2205.13220⟩.

[24] HASTIE, T.; TIBSHIRANI, R.; FRIEDMAN, J. *The Elements of Statistical Learning: Data Mining, Inference, and Prediction*. 2. ed. New York: Springer, 2009. ISBN 9780387848570.

[25] HAN, J.; KAMBER, M.; PEI, J. *Data Mining: Concepts and Techniques*. 3. ed. Waltham, Massachusetts: Morgan Kaufmann, 2011. ISBN 978-0-12-381479-1.

[26] HUANG, Z. Extensions to the k-means algorithm for clustering large data sets with categorical values. *Data Mining and Knowledge Discovery*, v. 2, n. 3, p. 283–304, 1998.

[27] AGGARWAL, C. C.; REDDY, C. K. (Ed.). *Data Clustering: Algorithms and Applications*. [S.l.]: Chapman & HallCRC, 2014. ISBN 978-1-4665-5821-2.

[28] KOPP, G. H. et al. Population genetic insights into the social organization of guinea baboons (papio papio): Evidence for female-biased dispersal. *American Journal of Primatology*, Wiley, v. 77, n. 8, p. 878–889, abr. 2015. ISSN 1098-2345. Disponível em: ⟨http://dx.doi.org/10.1002/ajp.22415⟩.

[29] MACHANDA, Z. P.; ROSATI, A. G. Shifting sociality during primate ageing. *Philosophical Transactions of the Royal Society B: Biological Sciences*, The Royal Society, v. 375, n. 1811, p. 20190620, set. 2020. ISSN 1471-2970. Disponível em: ⟨http://dx.doi.org/10.1098/rstb.2019.0620⟩.